

Three-ring mesogens containing *p*-carboranes: characterization and comparison with the hydrocarbon analogs in the pure state and as additives to a ferroelectric mixture

Adam Januszko,^a Piotr Kaszynski,*^a Michael D. Wand,^b Kundalika M. More,^b Serhii Pakhomov^a and Matthew O'Neill^b

^aOrganic Materials Research Group, Department of Chemistry, Vanderbilt University, Box 1822 Station B, Nashville, TN 37235, USA. E-mail: PIOTR@ctrvax.vanderbilt.edu

^bDisplaytech Inc., Longmont, CO 80503, USA

Received 12th September 2003, Accepted 15th January 2004

First published as an Advance Article on the web 15th March 2004

A series of sixteen three-ring esters of carboxylic acids derived from *p*-carborane, bicyclo[2.2.2]octane and benzene were synthesized and their mesogenic properties investigated using polarizing microscopy and DSC. The stability of the nematic phases follows the order BCO > Ph > 12-vertex > 10-vertex (or C > D > A > B). The biphenol derivatives **1** and **2** show significantly more rich smectic behavior than the pyrimidinylphenol esters **3** and **4**. Most of the esters show the expected effect on FLC properties of a host mixture. The exceptions are BCO derivatives **2C** and **4C**, which significantly lower the normalized P_s , and the carborane derivative **4A** which significantly increased the normalized P_s and γ_s values. In contrast to the hydrocarbon analogs, carborane esters lower the tilt angle.

Introduction

Ferroelectric liquid crystals (FLCs) constitute an important class of electro-optical materials for fast-switching displays.^{1,2} Typically, commercial FLCs are multicomponent mixtures in which desired properties³ are often finely tuned by using additives. Highly aromatic components tend to increase rotational viscosity and birefringence of the material, increasing its response time and making the manufacturing more difficult. These compounds are also often smectogenic and in high concentrations this may lead to the disappearance of the desired nematic phase in the mixture. In contrast, a number of heterocyclic compounds have been shown to have positive effects on FLC properties (such as a wide SmC phase, low melting point, low viscosity, and low birefringence) and are often used in mixture formulations.²

Our results for liquid crystals containing carborane rings **A** and **B** (Fig. 1) suggest that some of them may be useful additives for FLC mixtures. Generally, carborane derivatives are nematogenic,^{4,5} even more so than derivatives of bicyclo[2.2.2]octane (**C**), and also have relatively low birefringence.⁶ Both of these properties are desired for formulation of FLC mixtures, and this warrants investigations of the effect of carborane-containing mesogens on FLC properties.

To assess the effect of the carborane ring on liquid crystal properties, we focused on four series of structurally related three-ring esters **1–4** (Scheme 1) belonging to a general class of compounds used in FLC materials. The first three members of the series, **2A–2C**, have been reported earlier,⁷ and here we describe systematic studies of structural effects on mesogenic properties in four complete series.

The esters are derived from biphenol (**1** and **2**) and pyrimidinophenol (**3** and **4**) and contain an octyl chain connected to the

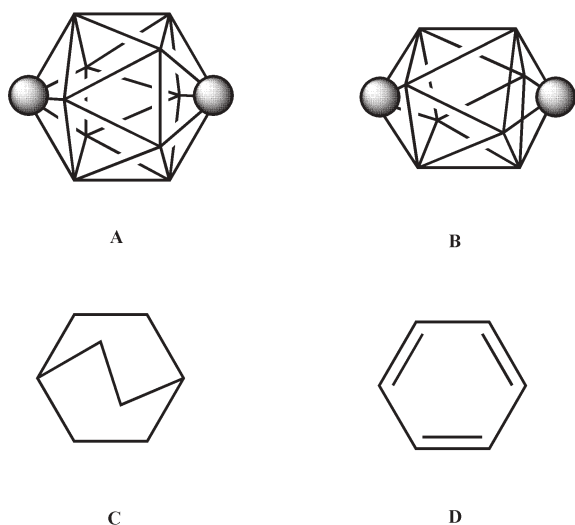
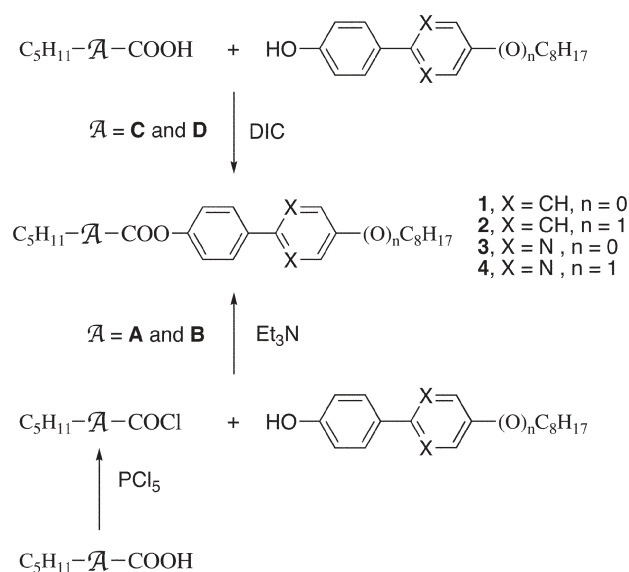


Fig. 1 1,12-Dicarbadoecaborane (12-vertex, **A**), 1,10-dicarbadoecaborane (10-vertex, **B**), bicyclo[2.2.2]octane (BCO, **C**) and benzene (Ph, **D**). In **A** and **B** each vertex corresponds to a BH fragment and the sphere represents a CH fragment.



Scheme 1

biaryl directly or through an oxygen atom. Both types of phenols have been used in the synthesis^{8,9} of FLCs, but the pyrimidinephenol system was found to be a particularly valuable intermediate.¹⁰ The phenols are esterified with carboxylic acids derived from the 12-vertex carborane (**A**), 10-vertex carborane (**B**), bicyclo[2.2.2]octane (**C**), and benzene (**D**) to form mesogens **1–4**. This allows for direct comparison of the effect of structural changes in the acid part as well as in the phenol part on the clearing temperature and the type and stability of smectic phases. Finally, several of these compounds were investigated as additives to FLC mixtures, and their effect on the tilt angle, rotational viscosity and spontaneous polarization was studied.

Results

Synthesis

Esters in series **C** and **D** were prepared by diisopropylcarbodiimide (DIC)-assisted esterification of carboxylic acids with appropriate phenols as shown in Scheme 1. The carbodiimide esterification did not work in the case of the carborane acids, and the esters **A** and **B** were obtained as was described earlier for the preparation of **2A–2C**.⁷ Thus carborane carboxylic acids were cleanly converted into acid chlorides using phosphorus pentachloride, and subsequently reacted with the appropriate phenol in the presence of a base (Scheme 1).

Thermal properties

The results of thermal analysis in Table 1 show that all compounds exhibit nematic phases with clearing temperatures above 120 °C. Generally, the order of clearing temperatures within each series is BCO > Ph > 12-vertex > 10-vertex (or **C** > **D** > **A** > **B**), and a graphical comparison of T_{NI} relative to the benzoate series **D** is shown in Fig. 2. Replacement of the benzene ring in the benzoate by the bicyclo[2.2.2]octane ring (**C**) significantly increases the clearing temperature by about 40 °C in each series **1–4**. The same substitution with carboranes decreases the T_{NI} by an average of 15 °C for the 12-vertex (**A**) and about 25 °C for the 10-vertex (**B**) carborane. The effect of the structural change appears to be qualitatively similar for all three cylindrical ring systems **A–C** relative to benzene series **D**: the T_{NIS} for the biphenyl series **1** and **2** are somewhat lower than those for the pyrimidinephenyl series **3** and **4**. Interestingly, the clearing temperatures for benzene (**D**) and 12-vertex carborane (**A**) derivatives of pyrimidinephenyl (series **3** and **4**) are almost the same.

The effect of structural changes in the biaryl core and the presence of a linking oxygen on the clearing temperatures are shown in Fig. 3. The replacement of two ring CH groups in the biphenyls **1** and **2** by nitrogen atoms in **3** and **4** has little effect on T_{NI} for 10-vertex (**B**) and BCO (**C**), but has a 10 °C stabilizing effect in 12-vertex (**A**) and a destabilizing effect in the benzoate (**D**) series. Incorporation of an oxygen atom between the octyl chain and the ring generally increases the clearing temperatures by about 25 °C. This coincides with an increased melting point in the biphenyl series **1** and **2**, and a decreased melting point in the pyrimidine series **3** and **4**.

The smectic behavior varies significantly between series of esters **1–4** but is consistent for each type of ring. In the biphenol series **1** and **2**, it is most pronounced for the BCO derivatives with the T_{SN} transition only about 30 °C below the T_{NI} . In the benzoates (series **D**) the nematic phase is about 50 °C wide, while in the carboranes the T_{SN} transition is 110 °C for the 10-vertex (series **B**) and 130 °C for the 12-vertex derivatives (series **A**) below the T_{NI} . This is consistent with the typically highly nematogenic behavior of carborane derivatives.^{4,5,11}

Generally, the pyrimidine derivatives **3** and **4** show only enantiotropic nematic phases. The exception is the BCO

derivative **3C** which shows a 5 °C wide enantiotropic smectic **B** phase. The benzoate derivatives **3D** and **4D** display monotropic **A** phases and the BCO ester **4C** exhibits a monotropic **G** phase. No smectic phases were found in the carborane derivatives of pyrimidinephenol even though the nematic phase was supercooled by about 10 °C (for series **A**) or 20 °C (series **B**) below the melting point.

In contrast, both biphenyl series **1** and **2** exhibit reach polymorphism with up to four smectic phases observed for the bicyclo[2.2.2]octane (**C**) and benzoate (**D**) derivatives as shown for **2D** in Fig. 4. All compounds except for **1C** and **2C** exhibit smectic **C** phases below the nematic. The benzoate derivatives **1D** and **2D** form enantiotropic phases, while the carborane derivatives exhibit monotropic **SmC** phases. In addition, the 10-vertex derivative **1B** displays a low temperature **SmG** phase at –4 °C. The bicyclo[2.2.2]octane derivative **2C** forms a smectic **A** phase before the **C** phase, while **1C** forms a smectic **B** which is followed by an **E** phase. Both benzene derivatives **1D** and **2D** exhibit the same sequence of tilted phases **C–I–F–G**. While all mesophases are enantiotropic for **1D**, the last three phases are monotropic and cover a narrow range for **2D** (Fig. 4).

The bicyclo[2.2.2]octane derivative **1C** exhibits two orthogonal phases **B** and **E**, while its octyloxy analog **2C** has two pairs of orthogonal-tilted phases: the high temperature **A–C** pair and the low temperature pair of ordered phases **B–G**.

The structure of smectic phases was identified based on characteristic textures and the established thermodynamic sequence of mesophases.^{12–14} The natural textures formed upon slow cooling of **1D** from the isotropic are shown in Fig. 5. Smectics **C**, **I** and **F** form Schlieren textures (Fig. 5a–c), while the **G** phase, grown from the Schlieren **F** phase, appears as a typical mosaic texture (Fig. 5d). Considering the number of observed lines, the texture in Fig. 5b is more consistent with the **SmF** (more lines) than with **SmI**. This assignment, however, is inconsistent with the order of the thermodynamic stability of smectic phases.

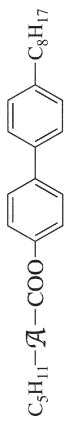
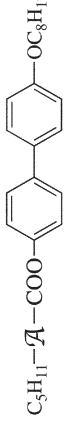
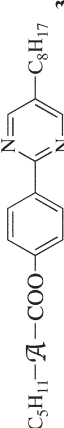
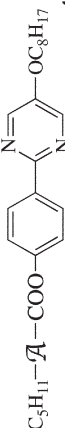
The assignment of the **SmB** phase in **1C** was difficult. The texture initially formed from the nematic phase was similar to that reported¹⁵ for **SmL** with its characteristic lancets in the pseudoisotropic background (Fig. 6a). After 30 min at constant temperature, the texture evolved into a typical **SmB** leaf-like texture (Fig. 6b). When the initial lancet texture was further cooled at a constant rate of 5 °C min^{–1}, a texture for **SmE** appeared (Fig. 6c) which after 30 min at constant temperature changed into a more characteristic texture shown in Fig. 6d.

The BCO derivative **2C** showed a strong tendency for a homeotropic alignment on an untreated glass surface. Thus the textures for the nematic and smectics **A** and **B** could not be observed. The smectic **C** showed up as a Schlieren texture and the smectic **G** appeared after 30 min at constant temperature from the homeotropic **S_B** as a typical mosaic texture shown in Fig. 7a. In our previous studies⁷ the **SmG** phase in **2C** could not be unambiguously identified and was designated as an **SmX** phase. For further support of the phase assignment and better observation of nematic and the orthogonal smectic phases **A** and **B**, the surface was covered with rubbed polyimide to impose a planar orientation on the sample. The smectic **A** phase formed from the nematic phase showed a fan-shaped texture which subsequently changed to the **C** phase (broken fan-shaped texture in Fig. 7b). The texture changed back to fan-shaped (edges regained focus) in the **B** phase (Fig. 7c). Further cooling resulted in the formation of the **G** phase, with characteristic stripes in the fan-shaped texture (Fig. 7d).

Effect on ferroelectric properties

Several mesogens were studied in a chiral FLC host mixture of phenylpyrimidines (MX 6146) and the results are shown in Table 2. As expected, all compounds increased the clearing

Table 1 Transition temperatures ($^{\circ}\text{C}$) and enthalpies (kJ mol^{-1}) for liquid crystals^a

		A		B		C		D								
																
1	Cr 50.5 (SmC 7)	N 139 I	Cr 56 (SmG -4)	SmC 18)	N 129 I	Cr ₁ 43	Cr ₂ 54	SmE 146	SmB 173	N 198 I	Cr 83	SmG 93.5	SmF 95	SmI 97	SmC 110	N 157 I
	19.0	0.2	22.9	1.2	0.4	10.1	15.7	3.3	0.7	0.1	18.2	0.3	0.0	2.5	1.8	1.3
2	Cr 80 (SmC 40)	N 167 I ^b	Cr 59 (SmC 46)	N 153 I ^b	Cr 68	SmG 93	SmB 130	SmC 144	SmA 185	N 219 I ^b	Cr 111	(SmG 106.2)	SmF 106.5	SmI 109)	SmC 134	N 186 I
	22.1	0.4	16.7	0.3	0.9	18.5	1.2	1.7	0.5	0.8	28.1	0.6	0.1	1.5	2.4	1.7
3	Cr ₁ 88	Cr ₂ 101	N 151 I	Cr 92	N 126 I	Cr 118	SmB 123	N 199 I			Cr 74	(SmA 48)	N 149 I			
	13.6	0.4	22.0	1.2	1.3	14.1	9.1	1.6			26.7	0.4	1.5			
4	Cr 104	N 175 I	Cr 79	N 152 I	Cr 100.5	(SmG 95.5)	N 222 I				Cr 67	(SmA 63)	N 177 I			
	29.6	2.5	21.8	1.4	28.8	8.0	1.8				29.1	0.9	2.1			

^a Cr-crystal, Sm-smectic, N-nematic, I-isotropic. ^b Ref: A. G. Douglass, K. Czuprynski, M. Mierzwa and P. Kaszynski, *Chem. Mater.* 1998, **10**, 2399-2402.

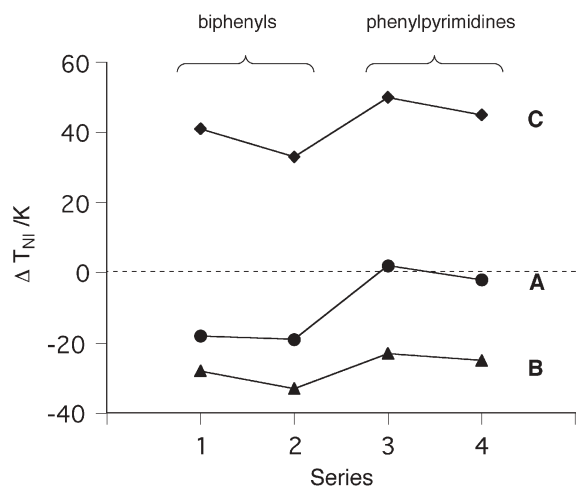


Fig. 2 T_{NI} s for the 12-vertex carborane derivatives (A, ●), 10-vertex carborane derivatives (B, ▲) and BCO (C, ◆) relative to the T_{NI} for the benzene derivatives D. The lines are guides for the eye.

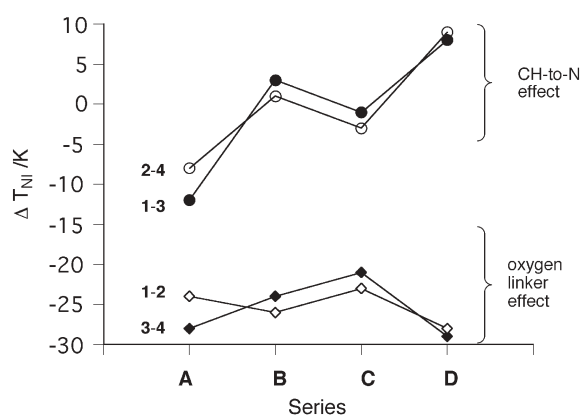


Fig. 3 The difference between the T_{NI} for the biphenols 1 and 2 (◇), pyrimidinephenols 3 and 4 (◆), biphenol 1 and pyrimidinephenol 3 (●), and biphenol 2 and pyrimidinephenol 4 (○). The lines are guides for the eye.

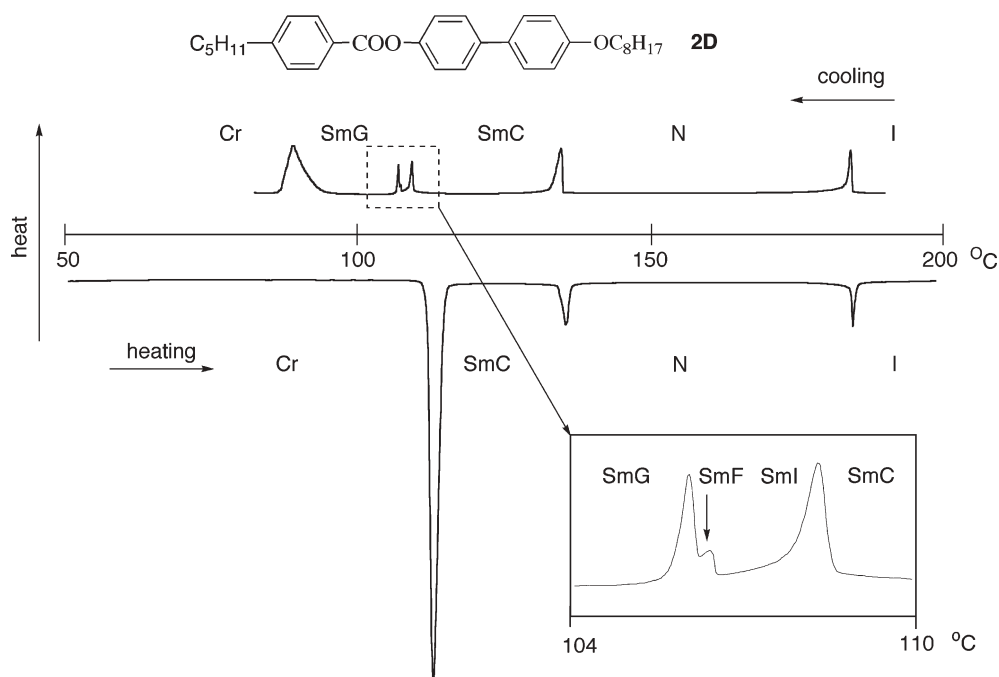


Fig. 4 DSC trace for **2D** obtained on heating (lower trace) and on cooling (upper trace) at a scanning rate of 5 °C min^{-1} . The expanded region of $104\text{--}110\text{ °C}$ is shown in the inset.

temperature of the mixture except for the carborane esters **3A** which practically had no effect on the N–I transition temperature. Generally, the effect on the clearing temperature of the dopants is approximately proportional to their clearing temperatures normalized by molecular weight (F_w). The only exception appears to be **2D** for which the observed increase in the mixture's T_{NI} is higher by about 8 °C than expected from the trend. Without **2D** the correlation factor R is 0.70.

The effect of the dopant on the stability of the mixture's smectic A phase can be related to the smectogenic tendency of the dopants. As in the case of the clearing temperatures, the T_{NA} of the mixture changes approximately proportionally to the normalized T_{NS} for the dopant. The exceptions are **2A**, which stabilized, and **3D**, which destabilized the A phase both by about 8 °C more than the trend indicates for the remaining compounds. Without **2A** and **3D** the correlation factor R for ΔT_{NA} and T_{NS}/F_w is 0.75. Generally, the most destabilizing effect on the S_A phase is exerted by octylpyrimidine derivatives **3** (Table 2), while the octyloxy analogs **4** have little effect on the N– S_A transition.

Unlike for the N–I and N–A transitions, there is no clear correlation between the properties of the dopants and the stability of the SmC^* phase of the mixtures. The derivatives of octyloxybiphenol **2**, which themselves exhibit a relatively stable smectic C phase (Table 1), have the most stabilizing effect on the SmC^* phase. Also, the octylpyrimidine derivatives **4C** and **4D** have a strong positive effect on the T_{AC} . In contrast, carborane derivatives of pyrimidines **3** and **4** appear to strongly destabilize the SmC^* phase by up to 14 °C for **3A**, and a similar effect is expected for **3B**. They also destabilize the SmA phase and this general behavior can be attributed to the lack of smectic behavior in the pure dopants (Table 1).

Results of electro-optical analysis for doped mixtures are shown in Table 2. Generally, all compounds, except for the bicyclo[2.2.2]octane derivative **1C**, increased the electric rise time τ .¹⁶ The largest increase of $270\text{ }\mu\text{s}$ was observed for the pyrimidine benzoates **3D** and **4D**. A relatively small increase in τ was measured for carborane derivatives **3A** and **3B** (*ca.* $100\text{ }\mu\text{s}$) and a particularly low value for the 12-vertex carborane derivative **4A** of only $45\text{ }\mu\text{s}$. These small increases in τ can be attributed, in part, to the decreased rotational viscosity¹⁷ γ_s for

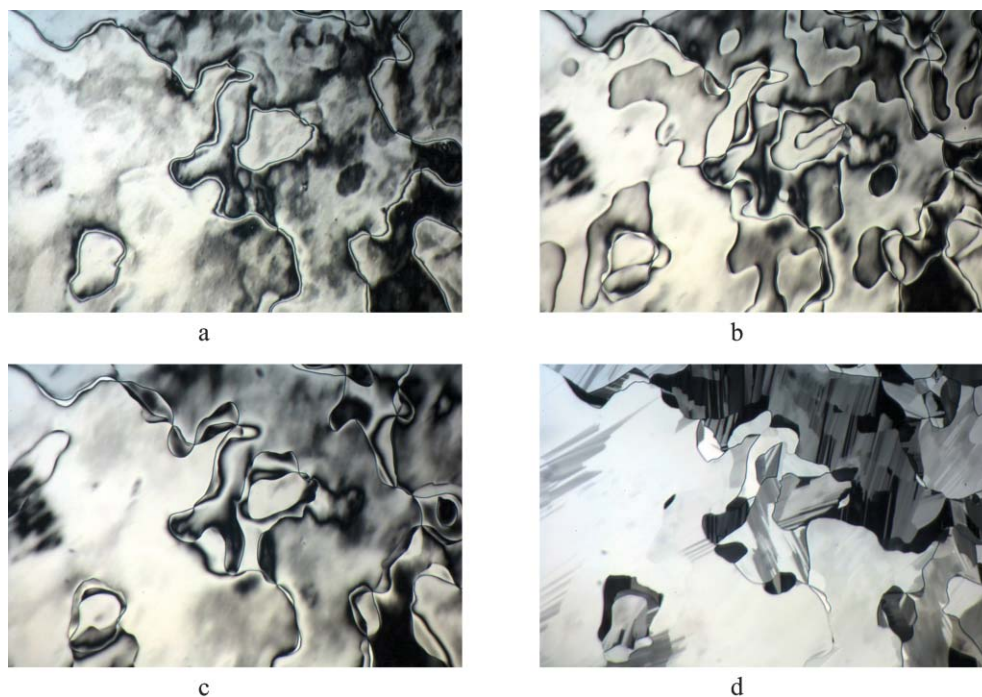


Fig. 5 Natural textures observed in polarized light for **1D** in the same sample region and approximately in the middle of the phase temperature range: a) Schlieren SmC; b) Schlieren SmI; c) Schlieren SmF; d) mosaic SmG. Magnification $60\times$.

these mixtures, by up to 26% for **3B**, which presumably overcompensates the significant decrease in spontaneous polarization P_s . The largest effect on viscosity was observed for the bicyclo[2.2.2]octane derivative **2C** and benzoate **3D** which increased the γ_s by 37 and 48%, respectively. Other compounds had either small positive or small negative effects on rotational viscosity.

The value of spontaneous polarization P_s was little affected by most of the dopants and the observed several percent decrease in P_s is consistent with diluting the FLC mixture with

a neutral achiral dopant. Exceptions are the carborane derivatives of pyrimidines **3** and **4** which significantly lowered the P_s value by 25–40%.

Optical measurements for the mixture showed that most of the compounds increased the tilt angle θ by up to 35° or about 6.5° for the bicyclo[2.2.2]octane derivatives **2C** and **4C**. Surprisingly, all four carborane derivatives of pyrimidines **3** and **4** markedly lowered the tilt angle θ , by up to about 6.6° or 34% for **3A**.

The electro-optical data in Table 2 show that the effect of the

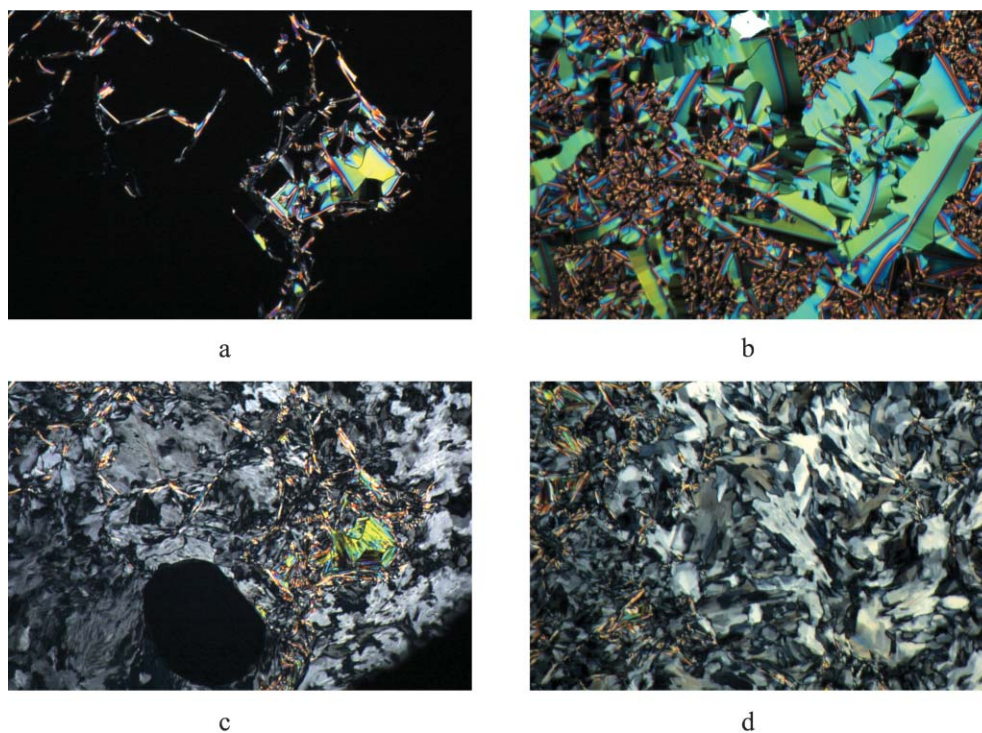


Fig. 6 Natural textures observed in polarized light for **1C** in the same sample region and approximately in the middle of the phase temperature range: a) initial SmB during cooling at 5 °C min^{-1} ; b) isothermally grown SmB (30 min); c) initial SmE during cooling at 5 °C min^{-1} ; d) isothermally grown SmE (30 min). Magnification $60\times$.

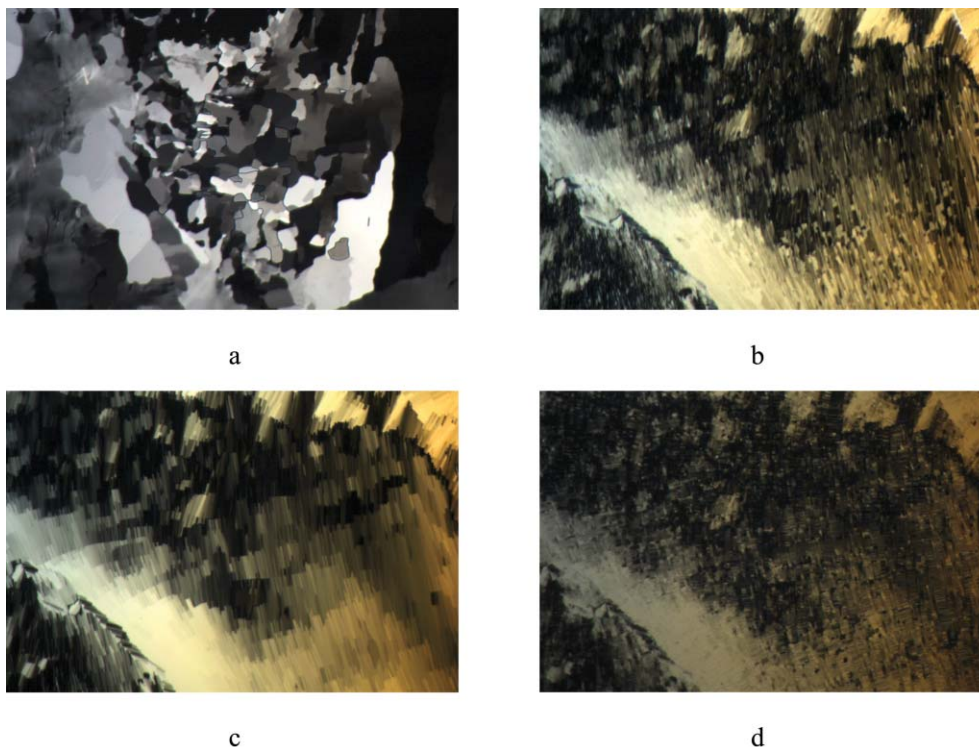


Fig. 7 Textures observed in polarized light for **2C** in the same sample region (b–c) and approximately in the middle of the phase temperature range: a) natural mosaic SmG; b) SmC on polyimide; c) SmB on polyimide; d) SmG on polyimide. Magnification $60\times$.

Table 2 Electro-optical data for 10% w/w solutions of selected compounds in a ferroelectric host MX 6146P^d

	$\Delta T_{IN}/K$	$\Delta T_{NA}/K$	$\Delta T_{AC}/K$	$\Delta\tau/\mu s$	$\Delta\gamma_s/mPa\ s$	$\Delta P_s/nC\ cm^{-2}$	$\Delta\theta/^\circ$
1B	4	-3	4	175 (74)	-1 (-2)	-0.3 (-4)	1.7 (9)
1C	9	4	-2	-15 (-6)	-4 (-9)	-0.3 (-4)	2.1 (11)
1D	4	-4	2	185 (79)	5 (11)	0.0 (0)	^b
2A	9	5	6	175 (74)	0 (0)	-0.3 (-4)	4.1 (21)
2C	9	2	6	127 (54)	17 (37)	-0.3 (-4)	6.7 (35)
2D	17	-1	9	^b	^b	^b	^b
3A	0	-4	-14	90 (38)	-10 (-22)	-3.0 (-42)	-3.6 (-19)
3B	1	-7	^b	110 (47)	-12 (-26)	-2.2 (-31)	-4.5 (-23)
3D	5	-12	-1	270 (115)	22 (48)	-0.5 (7)	^b
4A	4	0	-11	45 (19)	-6 (-13)	-1.9 (-26)	-6.6 (-34)
4B	4	0	-11	152 (65)	-10 (-22)	-2.1 (-29)	-3.2 (-17)
4C	7	-1	5	115 (49)	-6 (-13)	0.1 (1)	6.4 (33)
4D	10	-1	9	270 (115)	4 (9)	0.0 (0)	2.1 (11)

^a Change of clearing temperatures (ΔT_{IN}), nematic–smectic A transition (ΔT_{NA}), smectic A–smectic C* transition (ΔT_{AC}), electric rise time ($\Delta\tau$), rotational viscosity ($\Delta\gamma_s$), spontaneous polarization (ΔP_s) and tilt angle ($\Delta\theta$) upon addition of the depoant to the pure host. In parentheses, percentage change relative to the host: $\tau = 235 \pm 5\ \mu s$, $\gamma_s = 46 \pm 1\ mPa\ s$, $P_s = 7.2 \pm 0.1\ nC\ cm^{-2}$, $\theta = 19.2^\circ$. ^b Not measured.

carborane derivatives on the ferroelectric properties is different from that of the hydrocarbon analogs. Since the measured polarization and viscosity depend on the tilt angle, both values were normalized for comparison purposes, and the calculated P_s° and γ_1 values are shown in Table 3. The tilt-independent cone rotational viscosity γ_1 is calculated from the measured viscosity γ_s assuming the negligibly small contribution from the on-axis rotational viscosity γ_2 [eqn. (1)]. The normalization of the polarization also largely removed its dependence on temperature, which in any case should be small since the measurements were conducted at least 15 K below the C*–A transition.

$$\gamma_s = \gamma_1 \sin^2(\theta) + \gamma_2 \sin^2(\theta) \approx \gamma_1 \sin^2(\theta) \quad (1)$$

Data in Table 3 show that while most compounds have a small negative effect on P_s° of the mixture, there are two exceptions. Bicyclo[2.2.2]octane derivatives **C** significantly

Table 3 Normalized electro-optical data for 10% w/w solutions of selected compounds in a ferroelectric host MX 6146P^d

	$P_s/\sin(\theta)$	$\gamma_s/\sin^2(\theta)$
Host	19.9 ^b (0.0)	426 (0.0)
1B	19.3 (-0.6)	354 (-73)
1C	19.0 (-0.9)	381 (-108)
2A	14.4 (-2.5)	294 (-132)
2C	15.8 (-4.1)	330 (-96)
3A	19.3 (-0.6)	498 (+72)
3B	19.7 (-0.2)	522 (+96)
4A	24.3 (+4.4)	841 (+414)
4B	18.5 (-1.4)	469 (+42)
4C	16.9 (-3.0)	214 (-213)
4D	19.8 (-0.1)	383 (-44)

^a Spontaneous polarization and rotational viscosity normalized by the tilt angle. In parentheses, change relative to the host. ^b Value after addition of 10% of a neutral dopant to the host. Pure host value 21.9.

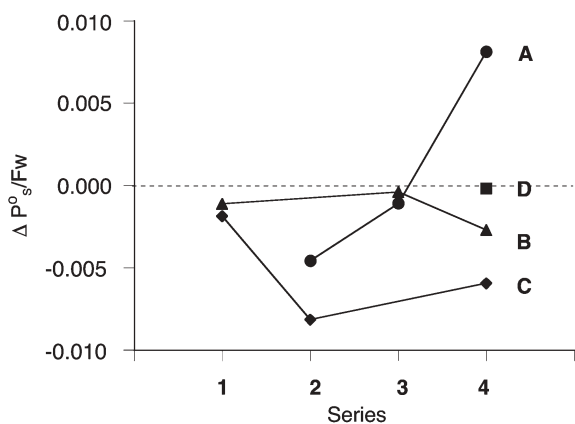


Fig. 8 Change in normalized spontaneous polarization normalized by molecular weight relative to $P_s^0 = 19.9 \text{ nC cm}^{-2}$ for a mixture with an ideal neutral dopant. The lines are guides for the eye.

decrease the polarization by up to about 20% for **2C**. On the other hand, addition of the carborane derivative **4A** increases the normalized spontaneous polarization by about 22%. At the same time, the rotational viscosity γ_1 for the latter mixture is significantly increased by about 100%, while for a mixture with bicyclo[2.2.2]octane derivatives **C**, γ_1 is lowered by a factor of 1/2.

Graphical analysis of data in Table 3 normalized further to account for molecular weight of the additives shows partial trends in the series of compounds (Fig. 8 and 9). Large molar values of ΔP_s^0 are observed for carborane and benzoate derivatives in **4A** and **4D** (Fig. 8). Partial data for other series indicate that the octyloxybiphenol esters **2** have the most detrimental effect on spontaneous polarization. The remaining two series **1** and **3** show a moderate effect on P_s^0 .

Similar analysis for the normalized change of viscosity $\Delta\gamma_1$ demonstrates a large molecular effect of carborane derivatives of pyrimidines **3** and **4** (Fig. 9) on the mixture's viscosity. In contrast, series **1** and **2**, and also bicyclo[2.2.2]octane derivatives, show a relatively low molar contribution to the material's viscosity.

Discussion and conclusions

All derivatives of carboranes **A** and **B** show a low tendency to form lamellar phases. While only low-temperature monotropic phases were observed for carboranes in series **1** and **2**, the hydrocarbon analogs exhibit up to four enantiotropic phases with the highest stability in bicyclo[2.2.2]octane derivatives **C**. This significant difference in thermotropic behavior of these

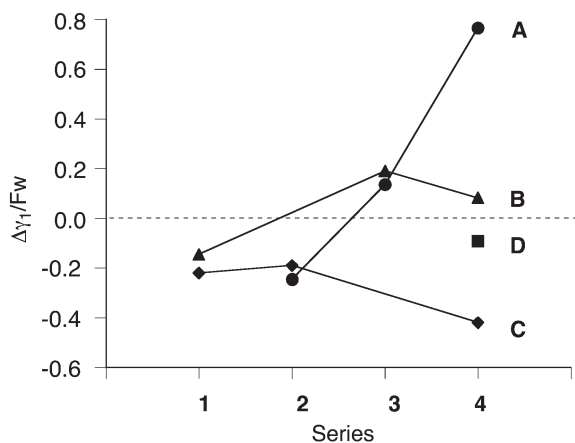


Fig. 9 Change in normalized rotational viscosity normalized by molecular weight relative to $\gamma_1 = 430 \text{ mPa s}$ for the pure mixture. The lines are guides for the eye.

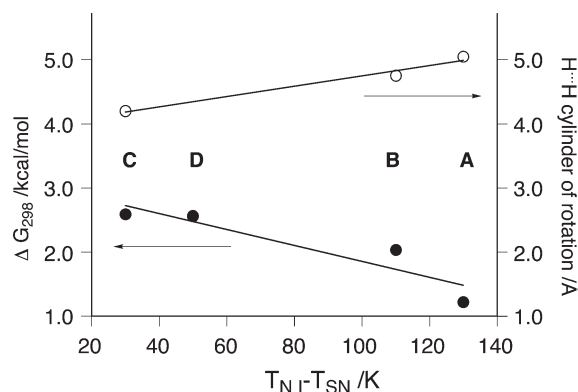


Fig. 10 Correlation of the average width of the nematic phase ($T_{NI} - T_{SN}$) for biphenols **1** and **2** and the ring width (○) and lowest barrier to internal rotation ΔG_{298} (●). The free energy of activation was obtained from MP2/6-31G(d) calculations with B3LYP/6-31G(d) thermodynamic corrections using Gaussian 98 suite of programs.

structurally closely related compounds may be due to either the static or the dynamic aspect ratio. The former takes into account the size of individual components and their distribution of conformational minima, while the latter also depends on the molecular rigidity and the height of barriers to internal bond rotation.

The significant difference in the stability of the smectic phases can be related to the large size⁷ of carboranes relative to BCO and benzene and hence to the difference in packing of their derivatives in the smectic phase. In fact, the width of the nematic phase ($T_{NI} - T_{SN}$) in series **1** and **2** increases proportionally to the width of three cylindrical rings **A–C** (Fig. 10). The trend in the width of the nematic phase also follows the trend in conformational mobility differences in series **1** and **2** defined by the lower of the two rotational barriers: around the alkyl-ring^{5,18} and ring $\text{C}=\text{O}$ bonds. The latter are usually lower than those for the alkyl-ring bonds, except for benzoate derivatives for which the $\text{Ph}-\text{CO}$ barrier is about $2.5 \times$ higher than the alkyl- Ph barrier. Thus, the conformational mobility in both benzoate and BCO derivatives is approximately the same, while it is higher for the 10-vertex and highest for 12-vertex carborane (Fig. 10). Lowering the barriers frees the motion of the alkyl chains, which lowers the dynamic aspect ratio and decreases the tendency to form an ordered phase.⁵ Thus, both static (ring size) and dynamic (conformational mobility) molecular characteristics reinforce each other in the lowering of the molecular aspect ratio and mesogenic behavior of the materials. Similar trends exist for the clearing temperatures T_{NI} , and this is consistent with our previous findings.⁵

The ability of the pure compounds to form nematic and smectic phases is also reflected in the effect on transition temperatures of the FLC mixtures. Generally, carborane derivatives destabilize the smectic phase except for **2A** which exhibits a relatively strong stabilization effect. This is consistent with our previous finding of unusual stabilization of a smectic E phase in a binary mixture of two structurally similar compounds.¹¹

Most of the compounds in the four series show a rather small molecular effect on mixture's spontaneous polarization and viscosity. It appears, however, that carborane derivatives **A** and **B** have greater positive effect on both mixture's characteristics, than the BCO series **C**. Among them, carborane **4A** shows an exceptional ability to significantly increase the polarization and viscosity.

The observed anomalous behavior of some carborane derivatives, especially the 12-vertex compound **A** in the FLC mixture, presumably arises from relatively strong intermolecular interactions between the dopant and the host. Such interactions may suppress molecular motions and result

in the formation of a more ordered phase and also higher P_s° and viscosity. In some sense, the addition of **4A** to the mixture is analogous to cooling the mixture to lower temperatures. These effects are consistent with our previous observations of the strong stabilization of smectic¹¹ and nematic phases,¹⁹ presumably due to interactions between the carborane and electron-rich benzene rings. These interactions may originate in the relatively high quadrupole moment of the carborane cage.⁵

Among the dopants, only the carborane derivatives lower the tilt angle, while the hydrocarbon analogs increase it and simultaneously lower the viscosity. This is presumably due to the poor packing properties and the larger size of the carborane rings in the more densely packed tilted phase than in the orthogonal one (the tilt of the smectic phase results in more efficient packing of molecules).

This unique combination of the ability to lower the tilt angle and the low birefringence in carborane derivatives is of interest for the formulation of mixtures with low tilt angle. For instance, FLC materials with an 11.25° tilt angle are useful for applications in which the light needs to be rotated a quarter wave. A common method for obtaining DC balance is to invert the image and turn the light off. If all the light needs to be preserved, this can be accomplished by using an FLC rotatable 1/4 wave plate. If the light is rotated a 1/4 wave by using an 11.25° tilt FLC material, then the inverted image is re-inverted creating a positive image, and the projection light can be turned on, thus doubling the efficiency of the FLC projector.²⁰

Further studies are necessary to better understand the effect of carborane-containing additives on FLC properties and the temperature dependence of the tilt angle and the viscosity.

Experimental section

NMR spectra were obtained at the 400 MHz (¹H spectra) and 128.4 MHz fields (¹¹B) in CDCl₃ and were referenced to TMS (¹H) or B(OMe)₃ set at 18.1 ppm (¹¹B). High resolution mass spectrometry (HRMS) was performed in the Notre Dame University Mass Spectroscopy Center. Elemental analysis was provided by Atlantic Microlab, Norcross, Georgia.

Optical microscopy and phase identification were performed using a PZO 'Biolar' polarized microscope equipped with a HCS250 Instec hot stage. Transition temperatures (onset) and enthalpies for pure compounds were obtained on a TA Instruments 2920 DSC using 2–3 mg samples and a heating rate of 5 °C min⁻¹ under a flow of nitrogen gas. Analogous measurements for the mixtures were run on a Mettler Toledo instrument. All solution studies were performed in a smectic C* host MX 6146P (Displaytech) using Automated Polarization Testbed III with the software version 4.2 (Displaytech) in a standard 4 μm cell at 26 °C, 6 V μm⁻¹ and 100 Hz. The tilt angle θ was measured as 1/2 of the rotation of the fully extinguished state between crossed polarizers in an electric field of 2.5 V μm⁻¹ and 1 Hz. The MX 6146P host had the following parameters: Cr -12 SmC* 55 SmA 69 N 76 I; $\tau = 235 \pm 3 \mu\text{s}$, $\gamma_s = 46 \pm 5 \text{ mPa s}$, $P_s = 7.2 \pm 0.2 \text{ nC cm}^{-2}$, $\theta = 19.2 \pm 0.2^\circ$. The error bars for the host represent typical accuracy of the measurement.

4-Pentylbenzoic and 4-pentylbicyclo[2.2.2]octane-1-carboxylic acids were purchased from Aldrich. 12-Pentyl-1,12-dicarbadodecaborane-1-carboxylic⁶ and 10-pentyl-1,10-dicarbadecaborane-1-carboxylic²¹ acids were obtained as described before. 4'-Octyl-4-biphenol, 4'-octyloxy-4-biphenol,²² 4-(5-octyl-2-pyrimidinyl)phenol,²³ and 4-(5-octyloxy-2-pyrimidinyl)phenol were obtained from Professor Roman Dabrowski (WAT, Warsaw, Poland).

Preparation of esters A and B. General procedure

A solution of the carborane carboxylic acid (0.2 mmol) and PCl₅ (42 mg, 0.2 mmol) in dry toluene (1 mL) was stirred at

40 °C for 30 min and the volatiles were removed under vacuum (10 min). The resulting oil was redissolved in dry toluene (1 mL), the appropriate phenol was added (0.20 mmol), followed by dry triethylamine (30 mg, 0.30 mmol). The reaction mixture was stirred at room temperature for 16 h, washed with water, and the organic layer extracted into ethyl acetate/hexanes (three times). The combined organic extracts were washed with brine, dried (MgSO₄) and the solvent removed *in vacuo*. The solid residue was purified by column chromatography (40 g of silica gel; eluted with 5% ethyl acetate in hexane) to yield a colorless solid, which was recrystallized from acetonitrile.

Preparation of esters C and D. General procedure

A solution of diisopropylcarbodiimide (30 mg, 0.24 mmol) in CH₂Cl₂ (1 mL) was added dropwise to a stirred solution of the appropriate phenol (0.20 mmol), carboxylic acid (0.2 mmol) and DMAP (2.4 mg, 0.02 mmol) in CH₂Cl₂ (2 mL). The reaction mixture was stirred at room temperature for 16 h, filtered, and the solvent removed *in vacuo*. The residue was purified by column chromatography (40 g of silica gel; eluted with 10% ethyl acetate in hexane) to yield a colorless solid, which was recrystallized from acetonitrile.

Each ester **A–D** was additionally purified by dissolving in CH₂Cl₂, filtering to remove particles, evaporating and recrystallizing from hexanes or a toluene/heptane mixture. The resulting crystals were dried under vacuum overnight at ambient temperature.

4'-Octyl-4-biphenyl 12-pentyl-1,12-dicarbadodecaborane-1-carboxylate (1A)

¹H NMR: δ 0.7–3.4 (m, 10H), 0.84 (t, $J = 7.3 \text{ Hz}$, 3H), 0.88 (t, $J = 7.3 \text{ Hz}$, 3H), 1.1–1.40 (m, 16H), 1.59–1.65 (m, 4H), 2.63 (t, $J = 7.6 \text{ Hz}$, 2H), 7.02 (d, $J = 8.6 \text{ Hz}$, 2H), 7.23 (d, $J = 8.0 \text{ Hz}$, 2H), 7.44 (d, $J = 8.0 \text{ Hz}$, 2H), 7.52 (d, $J = 8.6 \text{ Hz}$, 2H). ¹¹B NMR: δ -13.6 (d, $J = 157 \text{ Hz}$, 5B), -14.1 (d, $J = 157 \text{ Hz}$, 5B). HRMS (FAB⁺) m/z Calc. for C₂₈H₄₆B₁₀O₂ [M⁺]: 524.4428. Found: 524.4447. Anal. Calc. for C₂₈H₄₆B₁₀O₂: C, 64.33; H, 8.87. Found: C, 64.42; H, 8.87%.

4'-Octyl-4-biphenyl 10-pentyl-1,10-dicarbadecaborane-1-carboxylate (1B)

¹H NMR: δ 0.8–3.4 (m, 8H), 0.89 (t, $J = 6.7 \text{ Hz}$, 3H), 0.98 (t, $J = 7.0 \text{ Hz}$, 3H), 1.23–1.60 (m, 14H), 1.61–1.68 (m, 2H), 1.94–2.02 (m, 2H), 2.66 (t, $J = 7.8 \text{ Hz}$, 2H), 3.24 (t, $J = 8.3 \text{ Hz}$, 2H), 7.27 (d, $J = 7.7 \text{ Hz}$, 2H), 7.37 (d, $J = 8.5 \text{ Hz}$, 2H), 7.52 (d, $J = 8.0 \text{ Hz}$, 2H), 7.66 (d, $J = 8.6 \text{ Hz}$, 2H). ¹¹B NMR: δ -11.2 (d, $J = 155 \text{ Hz}$). HRMS (FAB⁺) m/z Calc. for C₂₈H₄₄B₈O₂ [M⁺]: 500.4086. Found: 500.4073. Anal. Calc. for C₂₈H₄₄B₈O₂: C, 67.38; H, 8.89. Found: C, 67.43; H, 8.99%.

4'-Octyl-4-biphenyl 4-pentylbicyclo[2.2.2]octane-1-carboxylate (1C)

¹H NMR: δ 0.88 (t, $J = 6.8 \text{ Hz}$, 3H), 0.89 (t, $J = 7.2 \text{ Hz}$, 3H), 1.15–1.40 (m, 18H), 1.44–1.48 (m, 6H), 1.60–1.66 (m, 2H), 1.92–1.96 (m, 6H), 2.63 (t, $J = 7.7 \text{ Hz}$, 2H), 7.08 (d, $J = 8.6 \text{ Hz}$, 2H), 7.23 (d, $J = 8.2 \text{ Hz}$, 2H), 7.47 (d, $J = 8.2 \text{ Hz}$, 2H), 7.55 (d, $J = 8.7 \text{ Hz}$, 2H). Anal. Calc. for C₃₄H₄₈O₂: C, 83.55; H, 9.90. Found: C, 83.74; H, 9.78%.

4'-Octyl-4-biphenyl 4-pentylbenzoate (1D)

¹H NMR: δ 0.89 (t, $J = 6.9 \text{ Hz}$, 3H), 0.91 (t, $J = 7.0 \text{ Hz}$, 3H), 1.25–1.40 (m, 14H), 1.61–1.71 (m, 4H), 2.65 (t, $J = 7.7 \text{ Hz}$, 2H), 2.71 (t, $J = 7.7 \text{ Hz}$, 2H), 7.26 (d, $J = 8.1 \text{ Hz}$, 2 Hz), 7.27 (d, $J = 8.6 \text{ Hz}$, 2H), 7.33 (d, $J = 8.2 \text{ Hz}$, 2H), 7.51 (d, $J = 8.2 \text{ Hz}$, 2H), 7.62 (d, $J = 8.6 \text{ Hz}$, 2H), 8.13 (d, $J = 8.2 \text{ Hz}$, 2H).

Anal. Calc. for C₃₂H₄₀O₂: C, 84.16; H, 8.83. Found: C, 83.62; H, 8.79%.

4-(5-Octyloxy-2-pyrimidinyl)phenyl 4-pentylbenzoate (2D)

¹H NMR: δ 0.90 (t, *J* = 7.0 Hz, 3H), 0.91 (t, *J* = 6.9 Hz, 3H), 1.23–1.53 (m, 14H), 1.63–1.71 (m, 2H), 1.77–1.84 (m, 2H), 2.71 (t, *J* = 7.7 Hz, 2H), 4.00 (t, *J* = 6.6 Hz, 2H), 6.97 (d, *J* = 8.8 Hz, 2H), 7.25 (d, *J* = 8.8 Hz, 2H), 7.33 (d, *J* = 8.4 Hz, 2H), 7.51 (d, *J* = 8.8 Hz, 2H), 7.59 (d, *J* = 8.7 Hz, 2H), 8.13 (d, *J* = 8.3 Hz, 2H). Anal. Calc. for C₃₂H₄₀O₃: C, 81.32; H, 8.53. Found: C, 81.08; H, 8.68%.

4-(5-Octyl-2-pyrimidinyl)phenyl 12-pentyl-1,12-dicarbodecaborane-1-carboxylate (3A)

¹H NMR: δ 0.8–3.4 (m, 10H), 0.84 (t, *J* = 7.3 Hz, 3H), 0.88 (t, *J* = 6.6 Hz, 3H), 1.05–1.40 (m, 16H), 1.60–1.66 (m, 4H), 2.61 (t, *J* = 7.5 Hz, 2H), 7.08 (d, *J* = 8.8 Hz, 2H), 8.40 (d, *J* = 8.8 Hz, 2H), 8.59 (s, 2H). ¹¹B NMR: δ –13.6 (d, *J* = 146 Hz, 5B), –14.1 (d, *J* = 147 Hz, 5B). HRMS (FAB⁺) *m/z* Calc. for C₂₆H₄₄B₁₀N₂O₂ [M⁺]: 526.4333. Found: 526.4364. Anal. Calc. for C₂₆H₄₄B₁₀N₂O₂: C, 59.51; H, 8.45. Found: C, 59.34; H, 8.43%.

4-(5-Octyl-2-pyrimidinyl)phenyl 10-pentyl-1,10-dicarbodecaborane-1-carboxylate (3B)

¹H NMR: δ 0.8–3.4 (m, 8H), 0.89 (t, *J* = 6.8 Hz, 3H), 0.98 (t, *J* = 7.1 Hz, 3H), 1.23–1.51 (m, 14H), 1.67 (quint., *J* = 7.3 Hz, 2H), 1.93–2.01 (m, 2H), 2.64 (t, *J* = 7.6 Hz, 2H), 3.24 (t, *J* = 8.3 Hz, 2H), 7.43 (d, *J* = 8.7 Hz, 2H), 8.53 (d, *J* = 8.7 Hz, 2H), 8.64 (s, 2H). ¹¹B NMR: δ –11.2 (d, *J* = 168 Hz). HRMS (FAB⁺) *m/z* Calc. for C₂₆H₄₃B₈N₂O₂ [M + H⁺]: 503.4069. Found: 503.4079. Anal. Calc. for C₂₆H₄₂B₈N₂O₂: C, 62.32; H, 8.45. Found: C, 62.11; H, 8.44%.

4-(5-Octyl-2-pyrimidinyl)phenyl 4-pentylbicyclo[2.2.2]octane-1-carboxylate (3C)

¹H NMR: δ 0.88 (t, *J* = 6.9 Hz, 3H), 0.89 (t, *J* = 7.2 Hz, 3H), 1.08–1.41 (m, 18H), 1.44–1.50 (m, 6H), 1.65 (quint., *J* = 7.2 Hz, 2H), 1.92–1.96 (m, 6H), 2.62 (t, *J* = 7.6 Hz, 2H), 7.15 (d, *J* = 8.8 Hz, 2H), 8.42 (d, *J* = 8.9 Hz, 2H), 8.60 (s, 2H). Anal. Calc. for C₃₂H₄₆N₂O₂: C, 78.32; H, 9.45. Found: C, 78.20; H, 9.50%.

4-(5-Octyl-2-pyrimidinyl)phenyl 4-pentylbenzoate (3D)

¹H NMR: δ 0.88 (t, *J* = 6.9 Hz, 3H), 0.91 (t, *J* = 7.0 Hz, 3H), 1.23–1.45 (m, 14H), 1.62–1.71 (m, 4H), 2.63 (t, *J* = 7.7 Hz, 2H), 2.71 (t, *J* = 7.7 Hz, 2H), 7.32 (t, *J* = 8.3 Hz, 2H), 7.33 (d, *J* = 8.8 Hz, 2H), 8.13 (d, *J* = 8.3 Hz, 2H), 8.49 (d, *J* = 8.8 Hz, 2H), 8.62 (s, 2H). Anal. Calc. for C₃₀H₃₈N₂O₂: C, 78.56; H, 8.35. Found: C, 78.42; H, 8.47%.

4-(5-Octyloxy-2-pyrimidinyl)phenyl 12-pentyl-1,12-dicarbodecaborane-1-carboxylate (4A)

¹H NMR: δ 1.0–3.3 (m, 10H), 0.84 (t, *J* = 7.3 Hz, 3H), 0.89 (t, *J* = 6.9 Hz, 3H), 1.05–1.43 (m, 14H), 1.48 (quint., *J* = 7.2 Hz, 2H), 1.63 (t, *J* = 8.2 Hz, 2H), 1.83 (quint., *J* = 7.0 Hz, 2H), 4.09 (t, *J* = 6.5 Hz, 2H), 7.06 (d, *J* = 8.9 Hz, 2H), 8.33 (d, *J* = 8.9 Hz, 2H), 8.42 (s, 2H). ¹¹B NMR: δ –13.6 (d, *J* = 162 Hz, 5B), –14.2 (d, *J* = 160 Hz, 5B). HRMS (FAB⁺) *m/z* Calc. for C₂₆H₄₅B₁₀N₂O₃ [M + H⁺]: 543.4361. Found: 543.4377. Anal. Calc. for C₂₆H₄₄B₁₀N₂O₃: C, 57.75; H, 8.20. Found: C, 57.62; H, 8.12%.

4-(5-Octyloxy-2-pyrimidinyl)phenyl 10-pentyl-1,10-dicarbodecaborane-1-carboxylate (4B)

¹H NMR: δ 0.8–3.4 (m, 8H), 0.90 (t, *J* = 6.8 Hz, 3H), 0.98 (t, *J* = 7.2 Hz, 3H), 1.20–1.75 (m, 14H), 1.85 (quint., *J* = 7.1 Hz, 2H), 1.97 (quint., *J* = 7.8 Hz, 2H), 3.24 (t, *J* = 8.3 Hz, 2H), 4.11 (t, *J* = 6.5 Hz, 2H), 7.41 (d, *J* = 8.7 Hz, 2H), 8.44–8.47 (m, 3H). ¹¹B NMR: δ –11.1 (d, *J* = 163 Hz). HRMS (FAB⁺) *m/z* Calc. for C₂₆H₄₂B₈N₂O₃ [M⁺]: 518.3940. Found: 518.3910. Anal. Calc. for C₂₆H₄₂B₈N₂O₃: C, 60.39; H, 8.19. Found: C, 60.42; H, 8.14%.

4-(5-Octyloxy-2-pyrimidinyl)phenyl 4-pentylbicyclo[2.2.2]octane-1-carboxylate (4C)

¹H NMR: δ 0.88 (t, *J* = 7.1 Hz, 3H), 0.89 (t, *J* = 7.0 Hz, 3H), 1.10–1.40 (m, 18H), 1.44–1.48 (m, 6H), 1.83 (quint., *J* = 7.0 Hz, 2H), 1.91–1.96 (m, 6H), 4.09 (t, *J* = 6.5 Hz, 2H), 7.13 (d, *J* = 8.8 Hz, 2H), 8.35 (d, *J* = 8.8 Hz, 2H), 8.43 (s, 2H). Anal. Calc. for C₃₂H₄₆N₂O₃: C, 75.85; H, 9.15. Found: C, 75.74; H, 9.16%.

4-(5-Octyloxy-2-pyrimidinyl)phenyl 4-pentylbenzoate (4D)

¹H NMR: δ 0.90 (t, *J* = 6.6 Hz, 3H), 0.91 (t, *J* = 6.7 Hz, 3H), 1.25–1.43 (m, 12H), 1.49 (quint., *J* = 7.4 Hz, 2H), 1.67 (quint., *J* = 7.4 Hz, 2H), 1.84 (quint., *J* = 7.0 Hz, 2H), 2.70 (t, *J* = 7.7 Hz, 2H), 4.10 (t, *J* = 6.5 Hz, 2H), 7.31 (d, *J* = 8.6 Hz, 2H), 7.32 (d, *J* = 8.1 Hz, 2H), 8.13 (d, *J* = 8.1 Hz, 2H), 8.42 (d, *J* = 8.5 Hz, 2H), 8.46 (s, 2H). Anal. Calc. for C₃₀H₃₈N₂O₃: C, 75.92; H, 8.07. Found: C, 76.00; H, 8.12%.

Acknowledgements

This project was supported in part by the National Science Foundation (DMR-9703002 and DMR-0111657) and The Petroleum Research Fund (28742-G1).

References

- 1 S. T. Lagerwall, in *Handbook of Liquid Crystals*, D. Demus, J. W. Goodby, G. W. Gray, H.-W. Spiess and V. Vill, ed., Wiley-VCH, New York, 1998, vol. 2B, pp. 515–664.
- 2 J. Dijon, in *Liquid Crystals, Applications and Uses*, B. Bahadur, ed., World Scientific, New Jersey, 1990, vol. 1, pp. 305–360.
- 3 T. Geelhaar, *Ferroelectrics*, 1988, **85**, 329–349.
- 4 P. Kaszynski and A. G. Douglass, *J. Organomet. Chem.*, 1999, **581**, 28–38.
- 5 W. Piecek, J. M. Kaufman and P. Kaszynski, *Liq. Cryst.*, 2003, **30**, 39–48.
- 6 A. G. Douglass, K. Czuprynski, M. Mierzwa and P. Kaszynski, *J. Mater. Chem.*, 1998, **8**, 2391–2398.
- 7 A. G. Douglass, K. Czuprynski, M. Mierzwa and P. Kaszynski, *Chem. Mater.*, 1998, **10**, 2399–2402.
- 8 T. Sakurai, N. Mikami, R.-i. Higuchi, M. Honma, M. Ozaki and K. Yoshino, *Chem. Commun.*, 1986, 978–979; Q. Wang, S. Y. Fan, H. N. C. Wong, Z. Li, B. M. Fung, R. J. Twieg and H. T. Nguyen, *Tetrahedron*, 1993, **49**, 619–638; D. S. Yufit, J. A. K. Howard and A. de Meijere, *Eur. J. Org. Chem.*, 2000, 4109–4117; K. A. Epstein, M. P. Keyes, M. D. Radcliffe and D. C. Snustad, *US Pat.*, 5,417,883, May 23, 1995.
- 9 S. M. Kelly, in *Handbook of Liquid Crystals*, D. Demus, J. W. Goodby, G. W. Gray, H.-W. Spiess and V. Vill, ed., Wiley-VCH, New York, 1998, vol. 2B, pp. 493–514.
- 10 M. D. Wand, W. N. Thurmes, R. T. Vohra, K. M. More, A. Yoshizawa, T. Hirai and J. Umezawa, *Mol. Cryst. Liq. Cryst.*, 1995, **263**, 217–222; K. Miyazawa, D. S. Yufit, J. A. K. Howard and A. de Meijere, *Eur. J. Org. Chem.*, 2000, 4109–4117; K. A. Epstein, M. P. Keyes, M. D. Radcliffe and D. C. Snustad, *US Pat.*, 5,417,883, May 23, 1995.
- 11 K. Czuprynski, A. G. Douglass, P. Kaszynski and W. Drzewinski, *Liq. Cryst.*, 1998, **26**, 261–269.
- 12 D. Demus and L. Richter, *Textures of Liquid Crystals*, 2nd edn., VEB Deutscher Verlag für Grundstoffindustrie, Leipzig, 1980.
- 13 G. W. Gray and J. W. Goodby, *Smectic Liquid Crystals – Textures and Structures*, Leonard Hill, Philadelphia, 1984.
- 14 J. W. Goodby, in *Handbook of Liquid Crystals*, D. Demus,

-
- J. W. Goodby, G. W. Gray, H.-W. Spiess and V. Vill, ed., Wiley-VCH, New York, 1998, vol. 2A, pp. 3–22.
- 15 K. Czuprynski, *Liq. Cryst.*, 1994, **16**, 399–403.
- 16 I. Dahl, S. T. Lagerwall and K. Skarp, *Phys. Rev. A*, 1987, **36**, 4380–4389.
- 17 C. Escher, T. Geelhaar and E. Boehm, *Liq. Cryst.*, 1988, **3**, 469–484.
- 18 P. Kaszynski, S. Pakhomov, K. F. Tesh and V. G. Young Jr., *Inorg. Chem.*, 2001, **40**, 6622–6631.
- 19 K. K. Kulikiewicz, A. Januszko, P. Kaszynski, A. G. Douglass, S. Pakhomov, R. W. Tilford and M. K. Patel, in preparation.
- 20 C. S. Park, M. Meadows and B. Koprowski, in *Microdisplay 2000*, Boulder, CO, September 2000, Abstract 16.1.
- 21 Z. Janoušek and P. Kaszynski, *Polyhedron*, 1999, **18**, 3517–3526.
- 22 B. Orzeszko, D. Melon-Ksyta and A. Orzeszko, *Synth. Commun.*, 2002, **32**, 3425–3429.
- 23 H. Zschke and R. Stolle, *Z. Chem.*, 1975, **15**, 441–443.